Underexpanded Sonic Jets: A PIV Study

K. Bülent Yüceil
Istanbul Technical University, Faculty of Aeronautics and Astronautics,
80626 Maslak, Istanbul, Turkey

M. Volkan Ötügen
Polytechnic University, Dept. of Mechanical, Aerospace & Manufacturing Engineering,
Six Metrotech Center, Brooklyn, NY 11201, USA

Engin Arik
Dantec Measurement Technology,
777 Corporate Dr., Mahwah, NJ 07430, USA

Abstract

The velocity field of underexpanded sonic air jets were investigated using digital particle image velocimetry (PIV). The jets were produced by a convergent nozzle connected to a settling chamber. Measurements were made for five different underexpanded jets with chamber-to-ambient pressure ratios of P_o/P_a=1.89, 4.77, 14.26, 29.36 and 38.41 (which correspond to fully-expanded jet Mach numbers M_j=1, 1.68, 2.38, 2.85 and 3.03, respectively). For each jet, streamwise and transverse velocities were obtained in the range x/D=0 and 8, D being the nozzle exit diameter. Mean velocities, turbulence intensities, turbulent shear stress and vorticity were obtained from 100 instantaneous PIV image pairs for each location. From these results the initial growth of the jets and the effect of underexpansion ratio on the flow structure was determined. Also, the effect of shock structure and shear layer growth on the mean velocity and turbulence fields were determined. It was found that the Mach disks that form in the near field of the highly-underexpanded jets significantly influence both the mean velocity the turbulence distributions. In general, the PIV method used provided good velocity data in the jet near field and allowed the identification of flow structures and their respective locations such as shock waves, expansion regions, slip lines and shear layers. However, the effect of particle inertia was evident just downstream of the Mach disk in the case of highly underexpanded jets.

Introduction

Sonic and supersonic jets are of interest from the point of view of fundamental fluid mechanics as well as practical applications. For example, a thorough understanding of the dynamics of these flows is important in the future development of air and space propulsion systems with high-performance nozzle designs. These nozzles are expected to provide not only improved thrust but also enhanced jet plume mixing for reduced thermal signature and environmental impact. However, detailed base line data on the structure of sonic and supersonic jets is needed for a range of operating pressures. Of particular interest is the structure of underexpanded jets. In these jets, the pressure at the nozzle exit is larger than that of the ambient. Such situations are encountered, for example, in rockets that operate through the atmosphere at varying altitudes. Another example is related to the power generation industry. The accidental discharge of a high-pressure gas into the atmosphere from a vessel through a small opening is an underexpanded sonic jet until the vessel pressure is has become sufficiently low.

Measurements in sonic/supersonic jets are difficult even for small-scale ground testing. In general, physical probes are not well suited for measurements in these flows as they can significantly alter the flow. Further, the quantity measured by the probe needs a certain interpretation in order to infer the actual property of the flow without the probe in place. Therefore, non-intrusive optical techniques are the preferred methods for the diagnostics of these flows. Further, laser-based optical techniques can be used to obtain time-frozen two-dimensional images of flow properties such as velocity, temperature and density. Recently, several techniques have been developed which show promise for the quantitative characterization of supersonic jets. For velocity, these include particle image velocimetry (Otugen et al., 1998; Wernet, 1997; Krothapalli et al, 1994; Lourenco and Krothapalli, 1988;), planar Doppler velocimetry (Clancy and Samimy, 1997; Clancy et al., 1998), filtered Rayleigh scattering (Miles and Lempert, 1990; Miles et al, 1994) and interferometric Rayleigh scattering (Seasholtz et al. 1992; Kouros and Seasholtz, 1994; Bivolaru et al., 1999).

The principles of the particle image velocimetry (PIV) technique have been described in numerous articles (see, for example, Adrian, 1991; Willert and Gharib, 1991). With the recent developments in real-time PIV, the technique has become an attractive velocity imaging method with a broad range of application. The technique has been routinely used for low speed flows providing two-component velocity information with reasonably good spatial resolution. Its application to high-speed supersonic flows, on the other hand, presents certain challenges. One of these challenges is associated with the inertia of particles used as scatters in the flow. Supersonic jet flows (unless ideally expanded) contain shock cells through which the flow accelerates and discelerate rapidly. Therefore, particles with larger mass and smaller slip drag cannot follow the flow with adequate fidelity. In the present study, special attention has been devoted to this problem. Porous silica particles have been used as scatteres in order to minimize the particle lag problem. These porous particles have a nominal diameter of 2.42 μm while their density is in the range between 0.18 and 2 gr/cm^3.

Experimental setup

Supersonic Jet Facility

A convergent nozzle with an exit diameter of D=8.9 mm provides the flow. The nozzle is connected to a settling chamber whose pressure can be varied. The jet uses dried air from a compressed air facility (Aerodynamic Research and Testing Facility at Polytechnic University). The jet can be run continuously for several hours before the compressed air facility has to be recharged. A pressure regulator placed upstream of the settling chamber controls the jet total (chamber) pressure. A seeding system introduces the special scattering particles into the jet fluid. The seeding system is composed of a high-pressure fluidized bed, containing the suspended seed particles, and a mixing chamber with multiple opposing jet injection ports. The mixing chamber is located approximately nine meters upstream of the jet settling chamber. The ambient air is seeded using a smoke generator. The settling chamber is instrumented with thermocouples and pressure transducers that provide information on jet total conditions. The general structure of the flow was determined prior to the PIV measurements by using Schieren and shadowgraph systems.

PIV system

In this project, a real-time PIV system was used. The PIV system consisted of a laser, light sheet optics, a cross-correlation video camera, a personal computer and a traversing system. The laser was a dual-cavity Nd:YAG laser, whose output was frequency doubled using a KDP crystal to obtain the 532 nm green line. The two laser cavities are inserted into a housing that contains optics to combine the two beams into one and then frequency double it. Each laser is operated in single Q–switch mode and signals generated by the synchronization module inside of the PIV processor control the firing of the laser cavities and hence the time interval between pulses. The laser output is formed into a light sheet and directed through the test area by using an assortment of mirrors and a cylindrical lens. The thickness of the light sheet at the measurement area is 1 mm. A cross-correlation camera is used to obtain the PIV images. The interrogation area was chosen to be 32 by 32 pixels and an overlap of 75% was used. The acquired images were processed in real time using a PIV processor. The system was controlled by a standard Pentium processor-based personal computer.

The laser, transmitting optics and the camera were all placed on a milling machine which was used as a manual traverse system. Therefore, the complete PIV system was traversed to obtain measurements at different regions of the stationary jet. The resolution of the traverse system was better than 0.1 mm in each direction. Further details of the optical system and the jet facility can be found in Otugen et al. (1998).

Experimental Results

In the present paper, velocity measurements in the initial jet region covering a streamwise distance of up to $x/D=8$ are be presented. The measurements were made for 5 different chamber pressures with the same sonic nozzle. The conditions for each jet studied are summarized in Table 1.

Table 1: Summary of experimental conditions

	P_o (kPa)	T_o (K)	P_e (kPa)	T_e (K)	P_o/P_a	P_e/P_a	M_j
Jet 1	191.50	282	101.33	235	1.89	1	1
Jet 2	483.32	282	255.73	235	4.77	2.52	1.68
Jet 3	1444.90	282	764.50	235	14.26	7.55	2.28
Jet 4	2974.90	282	1574.02	235	29.36	15.53	2.85
Jet 5	3891.89	282	2059.20	235	38.41	20.32	3.03

In the table, subscripts *o, e* and *a* refer to chamber, jet exit and ambient conditions, respectively. M_j is the equivalent (isentropically) fully expanded jet Mach number. Jet 1 in Table 1 is an ideally expanded sonic jet and it forms a baseline for comparison with the other underexpanded jets.
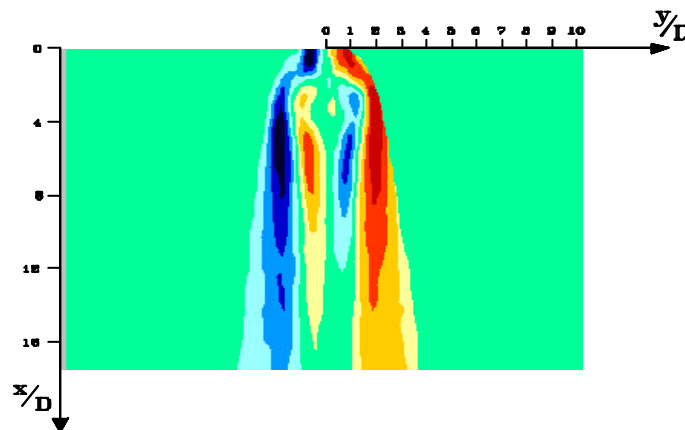

Fig. 1 : Vorticity distribution in Jet 5

In order to describe the general features of the highly-underexpanded sonic jet, the centerplane mean vorticity distribution for Jet 5(with $P_e/P_a = 20.32$) is shown in Fig 1. The flow field shown in the

figure extends from the nozzle exit to about x/D =17.5. The main features of the flow and their effect on the vorticity are evident. Immediately downstream of the nozzle, the jet starts to expand, adjusting to the ambient pressure of P_a = 1 atm. The vorticity distribution also indicates the presence of a Mach disk. The Mach disk is essentially a stationary normal shock wave that forms a certain axial distance from the nozzle exit. Upstream of it the flow is supersonic while, downstream, the flow is subsonic. The effect of the Mach disk and the slip lines downstream of it on the vorticity are clearly seen. The high-vorticity regions at the outer edges of the jet define the shear layer and as mixing takes place this outer shear layer grows in streamwise direction and the magnitude of vorticity decreases. At x/D ≈ 4, a second set of high-vorticity region forms inside the jet's outer boundary. This is caused by the slip line formed just downstream of the Mach disk. The flow inside the two inner lines is subsonic as it has just crossed a normal shock wave (the Mach disk). Just outside of these lines, however, the flow is still supersonic. The distance between the two inner lines of high-vorticity regions roughly defines the size of the Mach disk. Due to turbulent mixing, the slip line is quickly replaced by an inner mixing layer at a certain distance further downstream.

The centerline distributions mean streamwise velocity, u, normalized by the jet exit velocity, u_e, are shown in Figs. 2 through 6. In these figures, the mean lateral velocity, v, are also plotted to provide a rough assessment of the measurement accuracy. Indeed, as compared to the average magnitude of u, the deviation of v from zero is quite small for each case. When the jet is ideally expanded (Jet 1), the centerline streamwise velocity stays nearly constant up to about x/D = 5. Thereafter, shear layer penetrates the jet core and the centerline velocity starts decaying. Jet 2 shown in Fig. 3 is moderately underexpanded. The initial expansion region is characterized by the sharp increase in the streamwise velocity up to about x/D = 1. Through this initial expansion, the flow becomes supersonic with the streamwise velocity becoming nearly 40 percent larger than the exit value. Downstream of this point, a sharp drop in velocity is observed which is associated with a region of subsonic flow. Although Schlieren and shadowgraph visualizations do not clearly show a Mach disk for Jet 2, the velocity distribution hints at the existence of a Mach disk for this case. At this stage perhaps the disk is too small to be detected by the flow visualizations. Downstream of the disk, the flow again accelerates as it goes through a second expansion region. Further downstream, the centerline mean velocity fluctuates periodically with axial distance as it goes through the shock cell structure. This type of periodic velocity fluctuations in streamwise distance were also observed in slightly underexpanded Mach 1.6 supersonic jets using both the PIV technique (Otugen et al, 1998) and an interferometric Rayleigh scattering technique (Bivolaru, 1999). The centerline velocity in the initial expansion region for Jets 3, 4 and 5 (Figs. 4, 5 and 6, respectively) exhibit distributions similar to that for Jet 2. As the ratio P_e/P_a increases, the value of peak velocity also increases and the location of this peak shifts further downstream. These indicate higher centerline Mach numbers before the Mach disk and longer distances for the Mach disk location. For Jet 5 the maximum velocity is nearly double the exit velocity indicating a significant initial jet expansion and a divergence section through which the flow accelerates. Based on the measured maximum velocity and assuming isentropic flow at jet centerline up to the Mach disk, the centerline flow Mach number just upstream of the disk is estimated to be M ≈ 2.7 (which is, as expected, smaller than the fully-expanded M_j value of 3.03). This Mach number for Jets 2,3 and 4 are 1.5, 2.1 and 2.3, respectively.
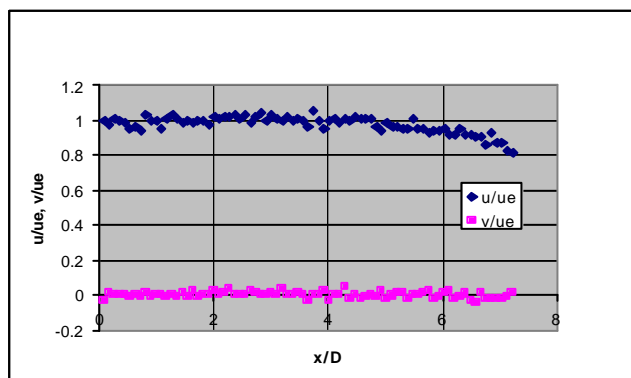

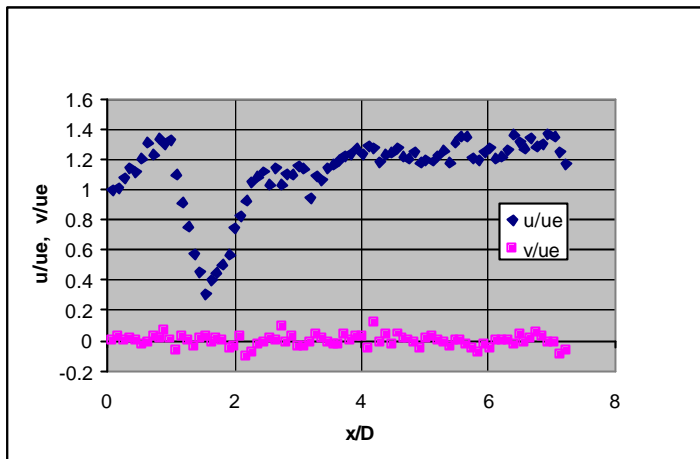**Fig. 2** : Mean streamwise and lateral velocity on jet axis for Jet 1

Fig. 3 : Mean streamwise and lateral velocity on jet axis for Jet 2
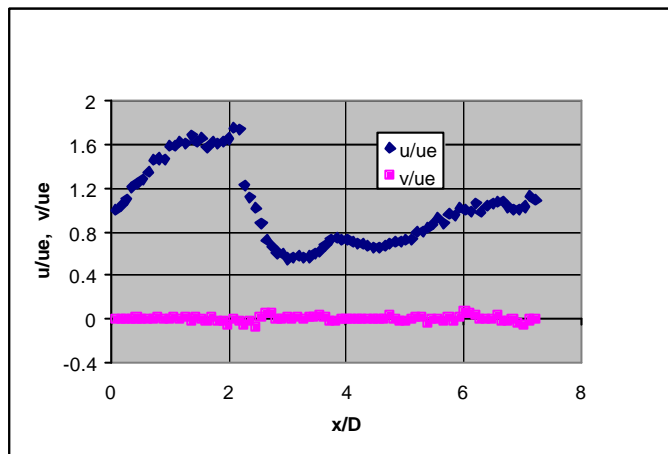

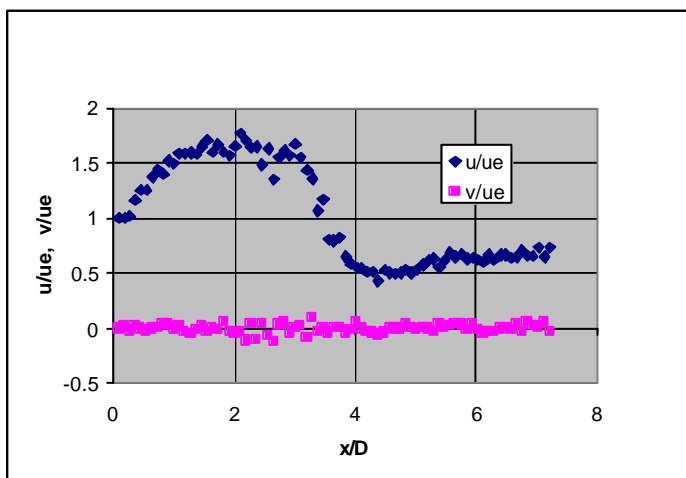**Fig. 4:** Mean streamwise and lateral velocity on jet axis for Jet 3

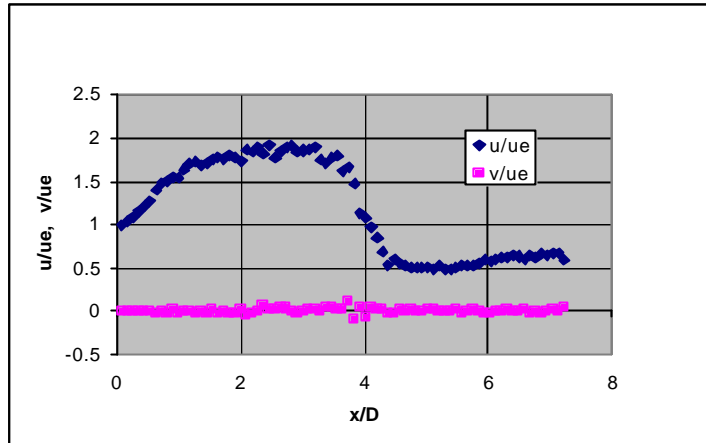**Fig. 5:** Mean streamwise and lateral velocity on jet axis for Jet 4

Fig. 6 : Mean streamwise and lateral velocity on jet axis for Jet 5

It is noted that the velocity drop across the normal shock (Mach disk) occurs with a finite (in fact one might term a "mild") gradient in all cases. For example, for Jet 5, the drop in velocity to the minimum level takes place over an axial distance of almost 0.8D. This is an indication that the measurement particles cannot follow the flow in high fidelity across the normal wave. However, the minimum velocity value downstream of the wave is very close to that calculated using Rankine-Hugoniot relations for a normal shock. Using the measured values upstream of the Mach disk, a downstream velocity of $u/u_e = 0.53$ is calculated for Jet 5. This value compares well with the measured value of $u/u_e = 0.51$.

The centerline distribution of turbulent streamwise and lateral velocity for all jets are presented in Figs. 7 through 11. Again, the rms of fluctuating velocity is normalized by the jet exit velocity, u_e. In general, the scatter in the data is significant. This is primarily due to the relatively small sample size for each measurement. One hundred PIV image pairs are used for the calculation of the rms values. Nevertheless, the data is useful in determining the relation of the basic flow structures such as shock waves with the turbulence field. On average, the streamwise component of the normal turbulent stress is larger than the lateral component. This is true for all jet cases studied. Clearly, isotropy of the turbulence field even on jet axis is not valid. Higher underexpansion ratios generally lead to higher overall turbulence levels. For Jets 3, 4 and 5, The turbulence levels increase with increasing distance from the nozzle reaching a maximum around the location of the Mach disk. Downstream of the disk, the levels drop sharply. The turbulence distributions show sharper peaks around Mach disk location as compared to the mean velocity
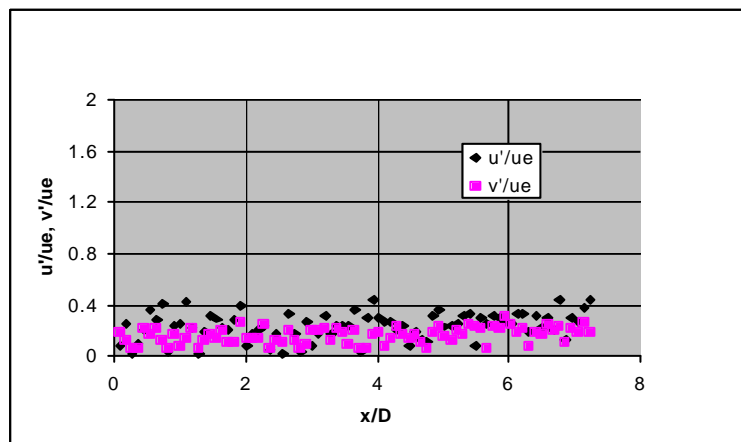

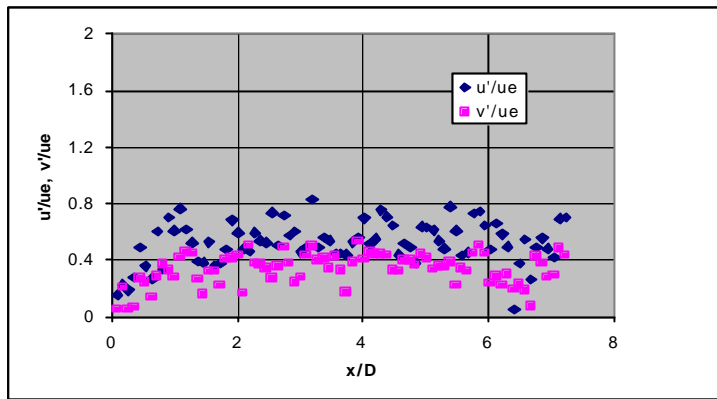**Fig. 7** : Streamwise and lateral turbulent velocity on jet axis for Jet 1

Fig. 8 : Streamwise and lateral turbulent velocity on jet axis for Jet 2
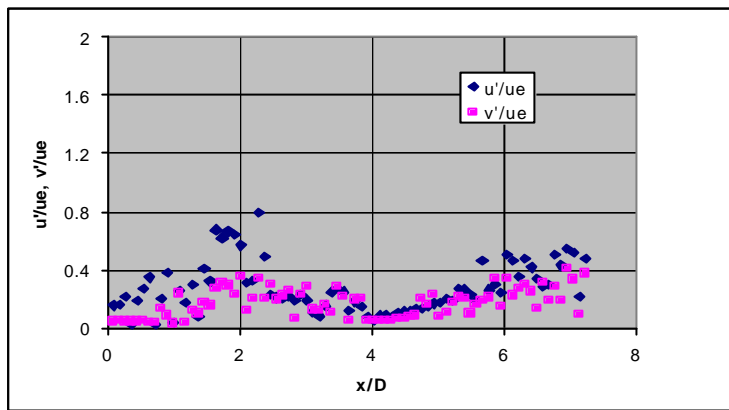

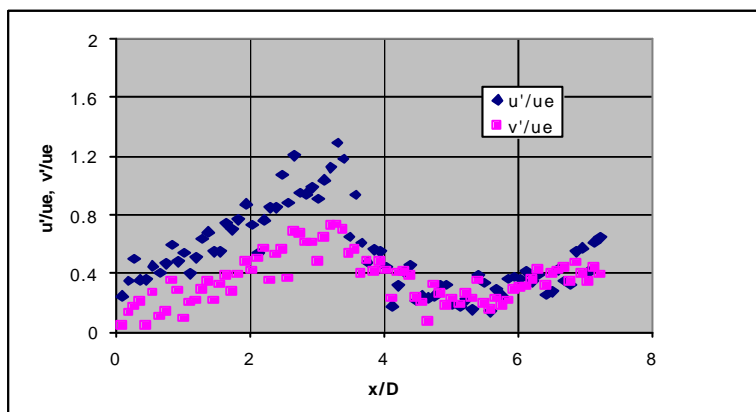**Fig. 9** : Streamwise and lateral turbulent velocity on jet axis for Jet 3

Fig. 10: Streamwise and lateral turbulent velocity on jet axis for Jet 4
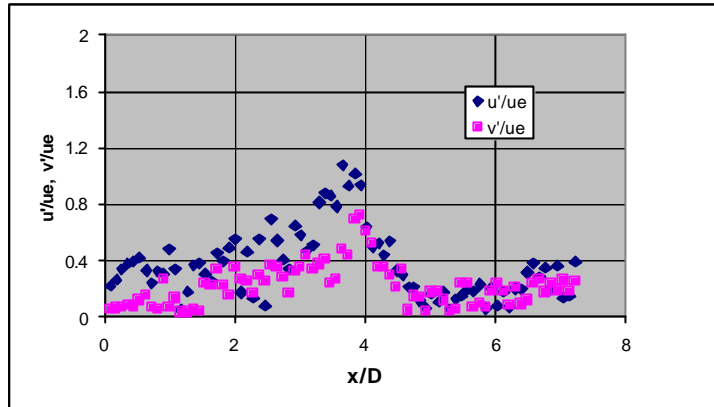
Fig. 11: Streamwise and lateral turbulent velocity on jet axis for Jet 5

distributions. Thus, the turbulence field may in fact be a better indicator of the <u>relative</u> location of the Mach disk. The use of this indicator as an absolute position locator for the disk may not be correct since a normal shock wave induces turbulence and the maximum levels may in fact occur slightly downstream of the shock wave. Further measurements and critical analysis are needed in order to clarify this point.

The transverse distributions of the mean streamwise and lateral velocity at x/D = 4.76 are presented in Figs. 12 and 13. This streamwise position is chosen for presentation since it is downstream of the Mach disk even for the jet with the largest underexpansion ratio (Jet 5). The effect of the Mach disk on the streamwise velocity is evident in Fig. 12. For the underexpanded jets, there is a clear dip in velocity at the centerline indicating the low velocity region downstream of the Mach disk. For the smaller underexpansion ratios, the Mach disk is smaller and it occurs at small axial distances from the nozzle. Therefore, by the axial distance of x/D = 4.76, the flow has re-accelerated and the velocity deficit is smaller and is confined to a narrower central portion of the flow for these jets. An interesting feature of these velocity profiles is that there are no uniform velocity regions and the gradients on the two sides of the peaks are relatively mild. Therefore, for all jets, by x/D = 4.76, the slip lines have deteriorated into mixing layers and the shear layers originally forming at the jet boundary have penetrated into the core of the jets. As for the lateral velocity distributions, in general, larger underexpansions lead to larger velocity magnitudes. On each side of the jets, the outer peaks/dips are due to the mass entrainment while the inner peaks are due to the jets' expansion.
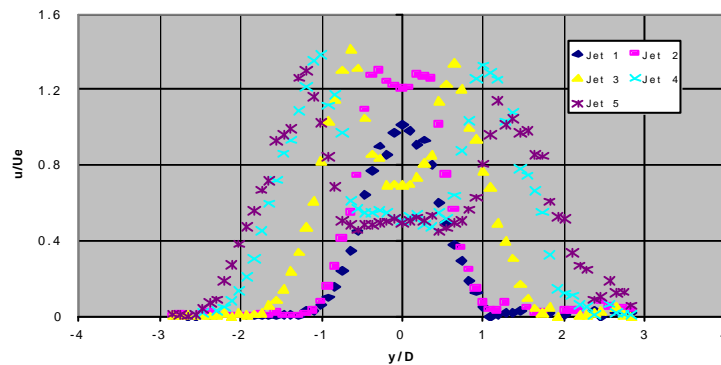

Fig. 12: Transverse distribution of mean streamwise velocity (x/D=4.76)
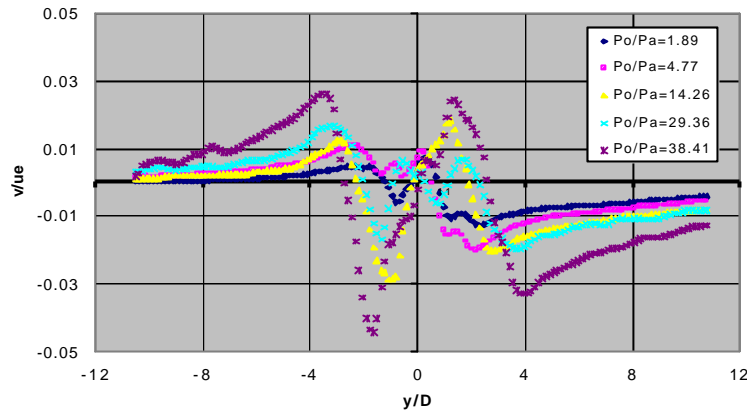
Fig. 13: Transverse distribution of mean lateral velocity (x/D=4.76)

The turbulent shear stress distributions for the same axial location are presented in Fig. 14. The occurrence of the maximum turbulence tends to correspond to the largest mean streamwise velocity gradient location. Overall, larger underexpansions lead to higher u'v' values at respective locations. Comparing Figs 12 to 14, it is also noted that the gradient transport relation is satisfied across the jets; throughout the profiles, the mean strain rate and turbulent shear stress carry opposite signs and the maximum absolute u'v' values closely correspond to the maximum mean shear. This is somewhat surprising since previous studies of incompressible turbulent jets indicate that the gradient transport relations are not always valid in the near field of those jets (Ferdman et al. 1999).
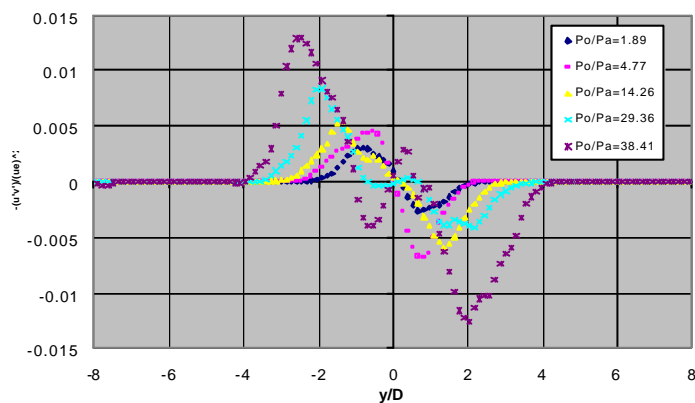

Fig. 14: Transverse distribution Reynolds shear stress (x/D=4.76)

Conclusions

The near field velocity structure of underexpanded sonic jets was studied using a digital PIV technique. The two main motivations were to investigate the applicability of the PIV technique to supersonic jet flows and to provide some basic velocity information on the near field of these jets. The PIV technique along with the particles used in this study, can indeed provide important information on the general structure of these jets and allow for some comparisons. However, particularly in the case of highly-underexpanded jets, the sudden and essentially discontinuous change in velocity across shock waves cannot be qualitatively measured by the PIV or, for that matter, any laser technique that relies on large particle (Mie) scattering. For example, the present measurements indicate a finite and, in fact, what may be termed a "mild" negative axial velocity gradient immediately downstream of the Mach disk. In reality, the change in velocity occurs across the thickness of the shock wave which is only a few gas mean free paths (Sukhomlinov et al., 2000). Nevertheless, the PIV measurements provide insightful information on the

velocity structure of these jets once it is understood that absolute magnitudes in the vicinity of strong shock waves may have relatively large errors. Of course, these types of measurements can be further improved with new particles with smaller mass-to-slip drag ratios. The study also shows that turbulence information can also be obtained using this measurement technique. The scatter in the turbulence data can be further improved by using larger number of frame pairs when calculating the statistics.

As expected, the velocity field of the underexpanded jet is dominated by the initial jet expansion and the subsequent formation of a Mach disk. However, turbulent mixing and the associated shear layer growth are also important factors in the initial region of these jets. For example, the slip lines that form immediately downstream of the Mach disk are rapidly destroyed by turbulent mixing in short axial distances from the disk. Also, even for the largest expansion ratio case of $P_e/P_a = 20.32$, the shear layer surrounding the jet seems to have penetrated a significant lateral distance and the whole jet is shearing with no apparent region of uniform velocity across it.

Acknowledgements

References

Adrian, R.J., *"Particle imaging techniques for experimental fluid mechanics"*, Ann. Rev. Fluid Mech. Vol. 23, pp 261-304, 1991.

Bivolaru, D., Otugen, M.V., Tzes, A. and Papadopoulos, G., *"Image processing for interferometric Mie and Rayleigh scattering velocity measurements"*, AIAA Journal, Vol. 37, No. 6, June 1999

Clancy, P.S., and Samimy, M., *"Two-Component laser Doppler velocimetry in high-speed flows,"* AIAA Journal, Vol. 35, pp. 1729-1738, Nov. 1997

Clancy, P.S., Samimy, M. and. Erskine, W.R., "*Planar Doppler Velocimetry: Three-component velocimetry in supersonic jets"*, 36th Aerospace Science Meeting and Exhibit, January 12-15, 1998, Reno, NV.

Ferdman, E, Otugen, M.V. and Kim, S, *"Effect of initial velocity profile on the development of round jets"*, Journal of Propulsion and Power, in press 1999.

Kouros, H. E. and Seasholtz, R.G., *"Fabry-Perot interferometer measurement of static temperature and velocity for ASTTOVL model tests"*, Symp. on Laser Anemometry: Advances and Applications, Ed: Otugen, M.V., Huang, T.T., (FED-Vol. 1, 1994)

Krothapalli, A, Whishart, L.M. and Lourenco, L.M., *"Nearfield structure of a supersonic jet: on-line PIV study"*, Proc. 7th International Symp. Appl. Laser Tech. Fluid Mech., Vol. 2, p26, Lisbon, Portugal, July 1994

Lourenco, L. M. and Krothapalli, A. *"Particle image displacement velocimetry measurements of a 3D jet"*, Physics of Fluids, Vol .31, No 07, July 1988, pp 1835-1837.

Miles, R.B., Lempert, R.W., *"Two dimensional measurement of density, velocity, and temperature, in turbulent high speed flows by UV Rayleigh scattering"*, Applied Physics B, Vol. 51, 1(1990).

Miles, R.B., Lempert, R.W., and Forkey, J., *"Instantaneous velocity fields and background suppression by filtered Rayleigh scattering"*, AIAA 29th Aerospace Sciences Meeting, Reno, NV. AIAA Paper No: 91-0357, 1991

Otugen, M. V., Bivolaru, D., Arik, E. and Jensen, K., *"PIV Study of a Mach 1.6 Supersonic Jet"* Proc. VSI_SPIE 98, December 6-9 1998, Yokohama, Japan.

Soukhomlinov, V.S., Kolosov, V.Y., Sheverev, V.A., Otugen, M.V*., "Formation and propagation of a shock wave in a gas with temperature gradients"*, Journal of Fluid Mechanics, April 2000, (under review)

Wernet, M.P. *"PIV for turbomachinery applications"*, Presented at the SPIE Conf. On Optical Diagnostics in Fluid and Thermal Flow, San Diego, CA, 1997 (NASA TM 107525)

Willert C. E. and Garib, M. *"Digital particle image velocimetry"*, Experiments in Fluids 10, 181-193, Springer-Verlag 1991.